J|A|C|S
ARTICLES

Published on Web 07/06/2009

Direct Electron Transfer to a Metalloenzyme Redox Center Coordinated to a Monolayer-Protected Cluster

Jose M. Abad,*,† Mhairi Gass,‡ Andrew Bleloch,‡ and David J. Schiffrin†

Chemistry Department, University of Liverpool, Liverpool L69 7ZD, United Kingdom, and UK SuperSTEM, Daresbury Laboratory, Daresbury, Cheshire WA4 4AD, United Kingdom

Received April 3, 2009; E-mail: J.Abad-Pastor@liv.ac.uk

Abstract: A strategy for establishing electrical contact to the metal center of a redox metalloenzyme, galactose oxidase (GOase), by coordination of a linker attached to a monolayer-protected gold cluster is presented. The cluster−enzyme hybrid system was first prepared in solution and characterized by high-angle annular dark-field scanning transmission electron microscopy. Electrochemical communication between a gold electrode and GOase was achieved by first modifying the electrode surface with a biphenyl dithiol self-assembled monolayer followed by reaction with gold clusters capped with thioctic acid. GOase was then immobilized by replacement of the H_2O molecule at the Cu^{II} exogenous site by coordination of a carboxylate-terminated gold cluster. This chemical attachment ensured electrical contact between the redox center and the electrode, leading to direct mediatorless electron transfer to the protein. Hybrid systems can find applications in biosensors and biofuel cells and for studying electrochemically the catalytic mechanism of reactions for which free radicals and electron-transfer reactions are involved. The present results can be extended to other metalloenzymes.

1. Introduction

Electron transfer (ET) in redox proteins plays a key role in many biological reactions, such as respiration and photosynthesis. Furthermore, direct protein ET between contacts is also of great interest for bioelectrocatalysis, bioelectronics, and biosensors and, more recently, in nanobiotechnology.[1,2] Redox enzymes, however, often lack direct electrical communication to electrode surfaces since their redox centers can be buried and insulated by the protein shell and, in addition, can be located too far from the electrode to display fast long-range ET rate constants. The use of nanoparticle−enzyme hybrid systems has recently been proposed[3] to overcome this problem by employing nanoparticles as nanoelectrodes to provide an electron relay pathway to the redox center region of the protein. Most of these approaches are based on a simple deposition of nanoparticles and enzymes on an electrode support.[4] Nonspecific molecular junctions have also been investigated recently employing molecular wires in conjunction with nanoparticles to connect electrodes to redox proteins' active centers.[5] These constructs differ considerably from traditional molecular wires by the inclusion of a nanoparticle within the molecular wire, and this approach has been shown recently to enhance ET rates by electrostatic binding of the carboxylate terminus of the nanoparticles employed to the lysine residues around the heme region in cytochrome *c*.[5b]

Key requirements for obtaining fast ET in nanoparticle−enzyme hybrid systems are to ensure short distances between the nanoparticle and the enzyme active site and to use a reproducible coupling method. The approaches commonly employed (nonspecific adsorption,[4,6a−c] covalent attachment[6d,e]) are difficult to control and can yield randomly bound proteins with poor orientation or inappropriate alignment of the redox center, thus resulting in inefficient ET to electrode surfaces. In addition, a suitable nanoparticle for integration into the protein must be employed. In most of the results reported, large nanoparticles have been used, and the protein has been immobilized on nanoparticles used as an extension of the electrode surface.[4,5b]

† University of Liverpool.
‡ Daresbury Laboratory.

(1) (a) Hagen, W. R. *Eur. J. Biochem.* **1989**, *182*, 523–530. (b) Armstrong, F. A.; Hill, H. A. O.; Walton, N. J. *Acc. Chem. Res.* **1988**, *21*, 407–413. (c) Heller, A. *Acc. Chem. Res.* **1990**, *23*, 128–134. (d) Frew, J. E.; Hill, H. A. O. *Eur. J. Biochem.* **1988**, *172*, 261–269. (e) Armstrong, F. A. *Curr. Opin. Chem. Biol.* **2005**, *9*, 110–117. (f) Léger, C.; Elliott, S. J.; Hoke, K. R.; Jeuken, L. J. C.; Jones, A. K.; Armstrong, F. A. *Biochem.* **2003**, *42*, 8653–8662. (g) Rudiger, O.; Abad, J. M.; Hatchikian, E. C.; Fernandez, V. M.; De Lacey, A. L. *J. Am. Chem. Soc.* **2005**, *127*, 16008–16009. (h) Blanford, C. F.; Heath, R. S.; Armstrong, F. A. *Chem. Commun.* **2007**, *17*, 1710–1712. (i) Shleev, S.; Tkac, J.; Christenson, A.; Ruzgas, T.; Yaropolov, A. I.; Whittaker, J. W.; Gorton, L. *Biosens. Bioelectron.* **2005**, *20*, 2517–2554. (j) Rahman, M. A.; Noh, H.; Shim, Y. *Anal. Chem.* **2008**, *80*, 8020–8027. (k) Scodeller, P.; Flexer, V.; Szamocki, R.; Calvo, E. J.; Tognalli, N.; Troiani, H.; Fainstein, A. *J. Am. Chem. Soc.* **2008**, *130*, 12690–12697.

(2) Gilardi, G.; Fantuzzi, A. *Trends Biotechnol.* **2001**, *19*, 468–476.

(3) (a) Willner, I.; Barnar, B.; Willner, B. *FEBS J.* **2007**, *274*, 302–309. (b) Willner, B.; Katz, E.; Willner, I. *Curr. Opin. Biotechnol.* **2006**, *17*, 589–596. (c) Katz, E.; Willner, I. *Angew. Chem., Int. Ed.* **2004**, *43*, 6042–6108. (d) Niemeyer, C. M. *Angew. Chem., Int. Ed.* **2001**, *40*, 4128–4158. (e) Katz, E.; Willner, I.; Wang, J. *J. Electroanal.* **2004**, *16*, 19–44. (f) Scott, D.; Toney, M.; Muzikr, M. *J. Am. Chem. Soc.* **2008**, *130*, 865–874.

(4) (a) Zhao, J.; O'Daly, J. P.; Henkens, R. W.; Stonehuerner, J.; Crumblisst, A. L. *Biosens. Bioelectron.* **1996**, *11*, 493–502. (b) Zhao, J.; O'Daly, J. P.; Henkens, R. W.; Stonehuerner, J.; Crumblisst, A. L. *J. Electroanal. Chem.* **1992**, *327*, 109–119. (c) Jia, J.; Wang, B.; Wu, A.; Cheng, G.; Li, Z.; Dong, S. *Anal. Chem.* **2002**, *74*, 2217–2223.

(5) (a) Zhang, J.; Kuznetsov, A. M.; Medvedev, I. G.; Chi, Q.; Albrecht, T.; Jensen, P. L.; Ulstrup, J. *Chem. Rev.* **2008**, *108*, 2737–2791. (b) Jensen, P. S.; Chi, Q.; Grumsen, F. B.; Abad, J. M.; Horsewell, A.; Schiffrin, D. J.; Ulstrup, J. *J. Phys. Chem. C* **2007**, *111*, 6124–6132.

The recognition chemistry by which nanoparticles can be used as a specific electron relay center to drive electrochemically redox proteins is a central problem in protein electrochemistry. An example of attempts to achieve specificity is the recent preparation of nanoparticle−enzyme hybrids that employs the reconstitution of the protein active site for the apo-flavoenzyme, apo-glucose oxidase, with a gold nanoparticle modified with its cofactor, *N*-(2-aminoethyl)-flavin adenine dinucleotide (FAD), that leads to an enhancement of the rate of ET to the enzyme.[7]

The present research develops a new concept to achieve both *specific recognition of a metallic redox center and enhancement of the electrical connectivity to an electrode* by using the coordination properties of the redox center of a metalloenzyme for its specific recognition by ligands attached to a gold cluster. The metal cluster acts, in this case, as an electron relay, thus achieving both specific functional recognition and an enhanced rate of ET. A functionalized monolayer-protected cluster (MPC) with suitable size to be coupled to the protein pocket has been employed to interact with the metal center.

The use of coordination chemistry for the attachment of proteins to nanoparticles has been recently explored. For example, a gold nanoparticle was linked to horseradish peroxidase by coordination of histidine groups in the protein to a cobalt complex containing a labile water molecule as one of the ligands attached to the metal ion and acting therefore as the recognition center.[8] The linking of nanoparticles using coordination chemistry principles has also been recently demonstrated by coupling silver nanoparticles functionalized with a nitrilotriacetic−Co^{II} complex to gold particles capped with imidazole thiol.[9] This latter work clearly demonstrated that the capping ligands of nanoparticles can be used for the construction of complex nanostructures.

Following from this previous work, we report here the direct electrical connection of the metal center of Galactose oxidase (GOase) by chemical coordination to a linker attached to a gold MPC acting as an electron relay center. The research strategy followed is schematically described in Figure 1a.

GOase (D-galactose, oxygen-6-oxidoreductase, EC 1.1.3.9, 68 kDa) was chosen for this study due to current interest in its catalytic mechanism involving a metallo−radical complex and the many potential biotechnological applications of this enzyme.[1g,10] GOase is a structurally simple radical−copper oxidase; it contains a single Cu site and catalyzes the two-electron stereospecific oxidation of primary alcohols to aldehydes by O_2 to produce H_2O_2.[10a−c,11] The enzyme consists of three domains, with the copper site lying close to the protein surface (~8 Å, Figure 1b). The copper center displays a square-pyramidal geometry coordinated by a stable tyrosyl radical (Tyr•272), two histidines (His496, His581), and a labile water molecule at the substrate-binding (exogenous) site in an equatorial position and a tyrosine (Tyr495) as the axial ligand (Figure 1b).[12] The redox-active species are the one-electron acceptors Cu^{II} ion and the tyrosyl radical (Tyr•272), which is cross-linked with a cysteine (Cys228), forming a tyrosyl-cysteine metalloradical active site. The redox chemistry involves three distinct states:[10a−c,11,13] a fully oxidized and active Cu^{II}-Tyr• state, an intermediate semioxidized and inactive form (Cu^{II}-Tyr)

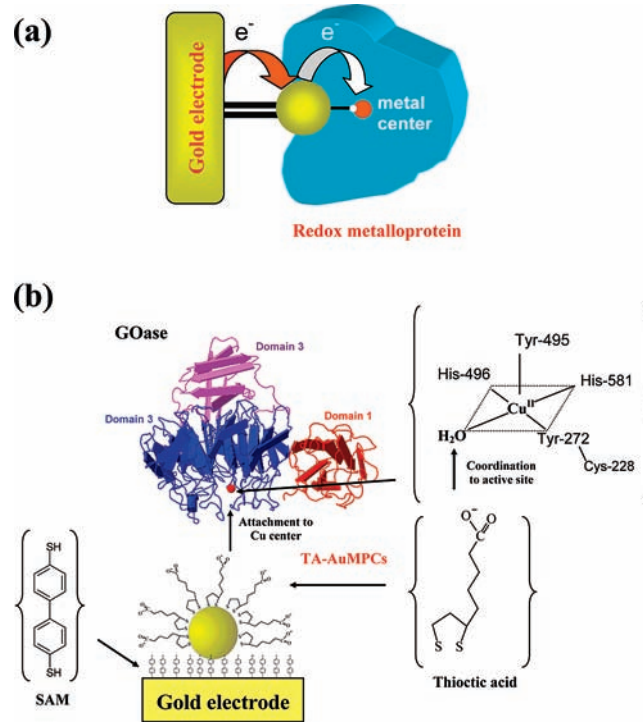

Figure 1. Direct electrical wiring of the metal center of a redox metalloenzyme by coordination of a linker attached to a gold nanoparticle. (a) Schematic description of a cluster−enzyme hybrid system. (b) Reaction strategy followed for the electrical connection of galactose oxidase (GOase) to a gold electrode.

(6) (a) Hayat, M. A. *Colloidal Gold: Principles, Methods and Applications*; Academic Press: New York, 1989 (three volumes). (b) Anand Gole, A.; Dash, C.; Soman, C.; Sainkar, S. R.; Rao, M.; Sastry, M. *Bioconjugate Chem.* **2001**, *12*, 684–690. (c) Mattoussi, H.; Mauro, J. M.; Goldman, E. R.; Anderson, G. P.; Sundar, V. C.; Mikulec, F. V.; Bawendi, M. G. *J. Am. Chem. Soc.* **2000**, *122*, 12142–12150. (d) Patel, N.; Davies, M. C.; Hartshorne, M.; Heaton, R. J.; Roberts, C. J.; Tendler, S. J. B.; Williams, P. M. *Langmuir* **1997**, *13*, 6485–6490. (e) Keating, C. D.; Kovaleski, K. M.; Natan, M. J. *J. Phys. Chem. B* **1998**, *102*, 9404–9413.

(7) Xiao, Y.; Patolsky, F.; Katz, E.; Hainfeld, J. F.; Willner, I. *Science* **2003**, *299*, 1877–1881.

(8) (a) Abad, J. M.; Mertens, S. F. L.; Pita, M.; Fernandez, V. M.; Schiffrin, D. J. *J. Am. Chem. Soc.* **2005**, *127*, 5689–5694. (b) Madoz-Gúrpide, J.; Abad, J. M.; Fernández-Recio, J.; Vélez, M.; Vázquez, L.; Gómez-Moreno, C.; Fernández, V. M. *J. Am. Chem. Soc.* **2000**, *122*, 9808–9817.

(9) Sendroiu, I. E.; Schiffrin, D. J.; Abad, J. M. *J. Phys. Chem. C* **2008**, *112*, 10100–10107.

(10) (a) Whittaker, J. W. *Chem. Rev.* **2003**, *103*, 2347–2363. (b) McPherson, M. J.; Parsons, M. R.; Spooner, R. K.; Wilmot, C. M. *Handbook of metalloproteins*; John Wiley & Sons, Ltd.: New York, 2001; Vol. 2, pp 1272−1283. (c) Whittaker, M. M.; Whittaker, J. W. *Biochemistry* **2001**, *40*, 7140–7148. (d) Rogers, M. S.; Dooley, D. M. *Curr. Opin. Chem. Biol.* **2003**, *7*, 189–196. (e) Sun, L.; Bulter, T.; Alcalde, M.; Petrounia, I. P.; Arnold, F. H. *ChemBioChem* **2002**, *8*, 781–783.

(11) (a) Whittaker, J. W.; Whittaker, M. M. *Pure Appl. Chem.* **1998**, *70*, 903–910. (b) Whittaker, J. W. *Arch. Biochem. Biophys.* **2005**, *433*, 227–239. (c) Baron, A. J.; Stevens, C.; Wilmot, C.; Seneviratnes, K. D.; Blakeley, V.; Dooleyfl, D. M.; Phillipsll, S. E. V.; Knowles, P. F.; McPherson, M. J. *J. Biol. Chem.* **1994**, *269*, 25095–25105. (d) Borman, C. D.; Saysell, C. G.; Wright, C.; Sykes, A. G. *Pure Appl. Chem.* **1998**, *70*, 897–902. (e) Whittaker, M. M.; Ballou, D. P.; Whittaker, J. W. *Biochemistry* **1998**, *37*, 8426–8436.

(12) (a) Ito, N.; Phillips, S. E. V.; Stevens, C.; Ogel, Z. B.; McPherson, M. J.; Keen, J. N.; Yadav, K. D. S.; Knowles, P. F. *Nature* **1991**, *350*, 87–90. (b) Ito, N.; Phillips, S. E. V.; Stevens, C.; Ogel, Z. B.; McPherson, M. J.; Keen, J. N.; Yadav, K. D. S.; Knowles, P. F. *Faraday Discuss.* **1992**, 75–84. (c) Ito, N.; Phillips, S. E. V.; Yadav, K. D. S.; Knowles, P. F. *J. Mol. Biol.* **1994**, *238*, 704–814.

(13) (a) Itoh, S.; Taki, M.; Fukuzumi, S. *Coord. Chem. Rev.* **2000**, *198*, 3–20. (b) Whittaker, M. M.; Whittaker, J. W. *J. Biol. Chem.* **1988**, *263*, 6074–6080. (c) Wachter, R. M.; Branchaud, B. P. *Biochim. Biophys. Acta* **1998**, *1384*, 43–54. (d) Saysell, C. G.; Borman, C. D.; Baron, A. J.; McPherson, M. J.; Sykes, A. G. *Inorg. Chem.* **1997**, *36*, 4520–4525. (e) Rothlisberger, U.; Carloni, P.; Doclo, K.; Parrinello, M. *J. Biol. Inorg. Chem.* **2000**, *5*, 236–250.

Scheme 1

$$\underset{(\mathrm{GOase_{ox}})}{\mathrm{Cu^{2+}\text{-}Tyr^{\bullet}}} \underset{-e^-}{\overset{+e}{\rightleftharpoons}} \underset{(\mathrm{GOase_{semi}})}{\mathrm{Cu^{2+}\text{-}Tyr^{-}}} \underset{-e^-}{\overset{+e}{\rightleftharpoons}} \underset{(\mathrm{GOase_{red}})}{\mathrm{Cu^{+}\text{-}Tyr}}$$

obtained after the reduction of the tyrosyl radical, and finally, a fully reduced and active state (Cu^{I}-Tyr) resulting from the reduction of Cu^{II} to Cu^{I} (Scheme 1).

The redox potentials of this enzyme have been obtained by spectroelectrochemical titrations with redox mediators since direct *reversible* electrochemical communication to an electrode has not been achieved,[13d,14,15] a general problem in enzyme electrochemistry.

The interconnection strategy followed is based on the introduction of a carboxylate-functionalized AuMPC of suitable size inside the copper pocket of the metalloprotein to achieve *direct coordination* with the metal center by replacement of the labile H_2O molecule at the Cu^{II} exogenous site (see Figure 1b), thus allowing a coordinatively electrical communication to an external electrode.[16] Thioctic acid-protected Au clusters (TA-AuMPCs) were linked to an electrode modified by a biphenyl dithiol self-assembled monolayer (SAM) (Figure 1b), and the GOase was then immobilized by coordination to the carboxylate-terminated clusters, thus providing the incorporation of a metal cluster within the electrode−protein connection.

The incorporation of a cluster into the protein metal center has been revealed by high-angle annular dark-field (HAADF) images obtained using spherical aberration-corrected scanning transmission electron microscopy (STEM).[17] The electrochemical properties of the hybrid systems have been studied by cyclic voltammetry.

2. Experimental Section

All chemicals were obtained from commercial sources and used as received. Milli-Q water (Millipore) was used throughout.

2.1. Synthesis of Gold Clusters Capped with a Thioctic Acid Monolayer (TA-AuMPCs). The clusters were prepared by the two-phase method of Brust et al.[18] Typically, $AuCl_4^-$ was transferred from an aqueous solution (6 mL, 30 mM, $HAuCl_4 \cdot 3H_2O$, Aldrich, 99.99%) to the organic phase using tetraoctylammonium bromide (TOABr) in toluene as the phase-transfer reagent (16 mL, 50 mM, Lancaster) with vigorous stirring for 30 min. Thioctic acid (TA, 1,2-dithiolane-3-pentanoic acid) (2 mL, 90 mM in toluene, Sigma) was then added to the two-phase mixture and stirred for another 30 min. A freshly prepared cooled aqueous solution of sodium borohydride (5 mL, 0.4 M, Aldrich) was rapidly added to the solution mixture at ~3 °C under vigorous stirring. The organic layer turned cloudy brown, and the mixture was left stirring for 3 h at ~3 °C. The clusters formed after reduction were soluble in the aqueous phase due to their carboxylate termination, and the organic phase was discarded. Size determination was carried out by HAADF-STEM microscopy as described below, and size distribution was estimated from size measurement of 200 clusters from the images obtained.

2.2. Gold Electrode Preparation. Polycrystalline gold disk electrodes (0.5 cm in diameter, 0.196 cm^2) were polished with 1 μm alumina powder (Buehler GmbH, Germany), rinsed, and sonicated for 15 min in Milli-Q water. The electrodes were then dipped in 0.1 M H_2SO_4 and activated by holding the potential at +2.0 V for 5 s and then at −0.35 V for 10 s, followed by potential cycling from −0.35 to +1.5 V at 4 V/s for 100 scans. Finally, the CV characteristic of a clean polycrystalline gold surface was recorded in 0.1 M H_2SO_4 at 0.1 V/s. The microscopic area was calculated by integration of the cathodic peak associated with the reduction of the gold oxide using a value of 482 $\mu C\ cm^{-2}$ for a monolayer of chemisorbed oxide on polycrystalline gold.[19] After the cleaning procedure, the gold electrodes were immersed for 24 h in a 1 mM solution of biphenyl-4,4′-dithiol (Aldrich) in ethanol. The electrodes were subsequently rinsed with ethanol and dried in air. Attachment of the TA-AuMPCs onto the modified biphenyl dithiol gold electrode was carried out by incubation of the electrode for 24 h in a 40 μM (concentration of clusters) colloidal aqueous solution of TA-AuMPCs obtained from the synthesis described above. The electrodes were subsequently washed with Milli-Q water.

2.3. Immobilization of GOase on Gold Electrodes Modified with Biphenyl Dithiol and [TA-AuMPCs]. Galactose oxidase (EC 1.1.3.9 from *Dactylium dendroides*, Sigma) was immobilized on gold electrodes modified with byphenyl dithiol-[TA-AuMPCs] by incubation for 1 h in a 1 mg/mL enzyme solution in 20 mM 2-(*N*-morpholino)ethanesulfonic acid (MES, Sigma) buffer, pH 5.1. This incubation time was considered appropriate based on our previous protein immobilization work.[8] The electrode was subsequently washed in 20 mM MES buffer, pH 7.5. A similar procedure was followed for the control experiment of GOase adsorption on gold electrodes modified only with a byphenyl dithiol SAM, i.e., when no clusters were present within the contacting molecular tether.

2.4. Electrochemical Measurements. Cyclic voltammetry data were obtained with an Autolab potentiostat (PGSTAT 10, Eco Chemie) using a three-electrode cell. Platinum gauze was used as counter electrode, and the potentials were measured with respect to a saturated calomel electrode (SCE). All solutions were deoxygenated by bubbling nitrogen for 30 min before the measurements, and all experiments were carried out at room temperature, 22 ± 2 °C. For the bioelectrocatalytic reduction of oxygen experiments, the solution was saturated with oxygen by bubbling pure oxygen for 15 min. The values of the formal potentials were calculated from the average of the anodic and cathodic peak potentials. For the pH dependence measurements, the pH was fixed with noninteracting buffers MES and 2-(*N*-cyclohexylamino)ethanesulfonic acid (CHES, Sigma).

2.5. High-Angle Annular Dark-Field Scanning Transmission Electron Microscopy (HAADF-STEM). Imaging of the enzyme and of the product of the reaction between GOase and TA-AuMPCs was carried out using the SuperSTEM facility at Daresbury Laboratory, UK. The SuperSTEM is a dedicated, aberration-corrected STEM instrument consisting of a 100 kV Vacuum Generators (VG) HB501field emission gun (FEG) instrument corrected to third order using a combination of dipole, quadrupole, and octupole elements. This technique is sensitive to the mass and thickness of the samples, and for relatively thin specimens the intensity increases linearly with sample thickness. The measured intensity is approximately proportional to the square of the atomic number, thus offering the possibility of studying atomic structures in detail.[17] For linking the gold clusters to the active site of the enzyme, a solution of 1 mg/mL of GOase (40 μL) in 20 mM of MES buffer, pH 5.1, was mixed with 10 μL of 40 μM TA-AuMPCs and left to react for 1 h. The samples were deposited onto TEM grids coated with a Lacey carbon film (Agar scientific, 400 mesh copper) and left to evaporate in air.

(14) Wright, C.; Sykes, A. G. *J. Inorg. Biochem.* **2001**, *85*, 237–243.
(15) (a) Johnson, J. M.; Halsall, H. B.; Heineman, W. R. *Biochemistry* **1985**, *24*, 1579–1585. (b) Tkac, J.; Vostiar, I.; Gemeiner, P.; Sturdik, E. *Bioelectrochemistry* **2002**, *56*, 23–25.
(16) Wright, C.; Im, S.-C.; Twitchett, M. B.; Saysell, C. G.; Sokolowski, A.; Sykes, A. G. *Inorg. Chem.* **2001**, *40*, 294–300.
(17) Ward, E. P. W.; Arslan, I.; Midgley, P. A.; Bleloch, A.; Thomas, J. M. *Chem. Commun.* **2005**, 5805–5807.
(18) Brust, M.; Walker, M.; Bethell, D.; Schiffrin, D. J.; Whyman, R. *J. Chem. Soc., Chem. Commun.* **1994**, 801–802.
(19) Oesch, U.; Janata, J. *Electrochim. Acta* **1983**, *28*, 1237–1246.

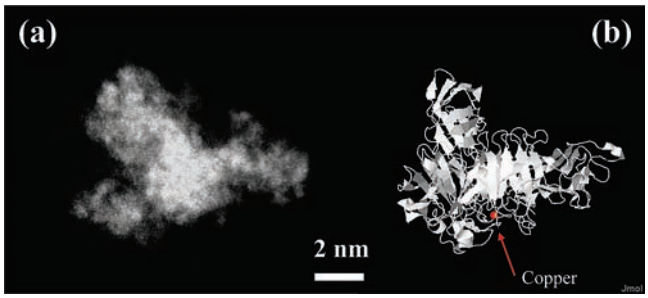

Figure 2. Comparison of a galactose oxidase image obtained by HAADF-STEM with a GOase model. (a) HAADF-STEM image. (b) 3D molecular display of the protein model obtained from Jmol, an open-source Java viewer for chemical structures in 3D (http://www.jmol.org/), used with PDB entries for GOase (2eie; 1gof in ref 12a) from the Protein Data Bank (www.pdb.org). The arrow indicates the position of the copper center.

3. Results and Discussion

3.1. Synthesis and Characterization of Cluster−Enzyme Hybrid System, AuMPC−GOase. Water-soluble functionalized carboxylate gold clusters were synthesized to obtain a size suitable for accessing the pocket at the copper site. From a molecular modeling analysis based on X-ray diffraction data,[12] an approximate cavity size of the copper site was estimated roughly as 1.6 nm. Thus, a requirement of the present strategy was the use of clusters smaller than this. The synthesis was carried out using a two-phase synthesis method,[18] since this yields better particle monodispersity and higher particle concentrations than water-based preparations. Thioctic acid was chosen as capping ligand in view of its lower pK_a value [pK_a(TA in solution) ∼5; pK_a(TA in a SAM) ∼6.5; this range of values was required for further protein coupling] and its better stability as previously reported.[8a,20] Cyclic disulfide SAMs are more stable than those obtained with single thiol or acyclic disulfide units, a consequence of the anchoring of the ligand to the metal core surface through two sulfur atoms. To prepare sufficiently monodisperse monolayer-protected gold clusters of the desired size, the Au:TA ratio and the temperature and rate at which the reaction is conducted were adjusted following the modifications proposed by Murray et al.[21] The mole ratio used varied from 1:1 to 1:5, and a low reaction temperature was employed. The best results were obtained for a 1:1 ratio. Aberration-corrected HAADF-STEM characterization of these TA-AuMPCs (Figure S1, Supporting Information) shows a narrow cluster size distribution with an average diameter of 1.4 ± 0.3 nm. The UV−vis spectrum (Figure S2, Supporting Information) did not show the characteristic plasmon band at 520 nm, confirming particle diameters below 2 nm.[22]

3.2. HAADF-STEM Study of the AuMPC−GOase Hybrids. The feasibility of coordination of the TA-capped gold clusters to the copper center was first studied by reacting in solution the functionalized clusters with the enzyme. The specific attachment achieved was studied by imaging the structures formed using HAADF-STEM. Figure 2 compares a HAADF-STEM image of the protein and a molecular model of GOase. The shape observed for the protein (Figure 2a) is in good agreement with the structure obtained from X-ray crystallography (Figure 2b), and the dimensions are close to those reported for the unit cell (98.0 × 89.4 × 86.7 Å).[12a] HAADF-STEM imaging provided good visualization of the protein in transmission mode.

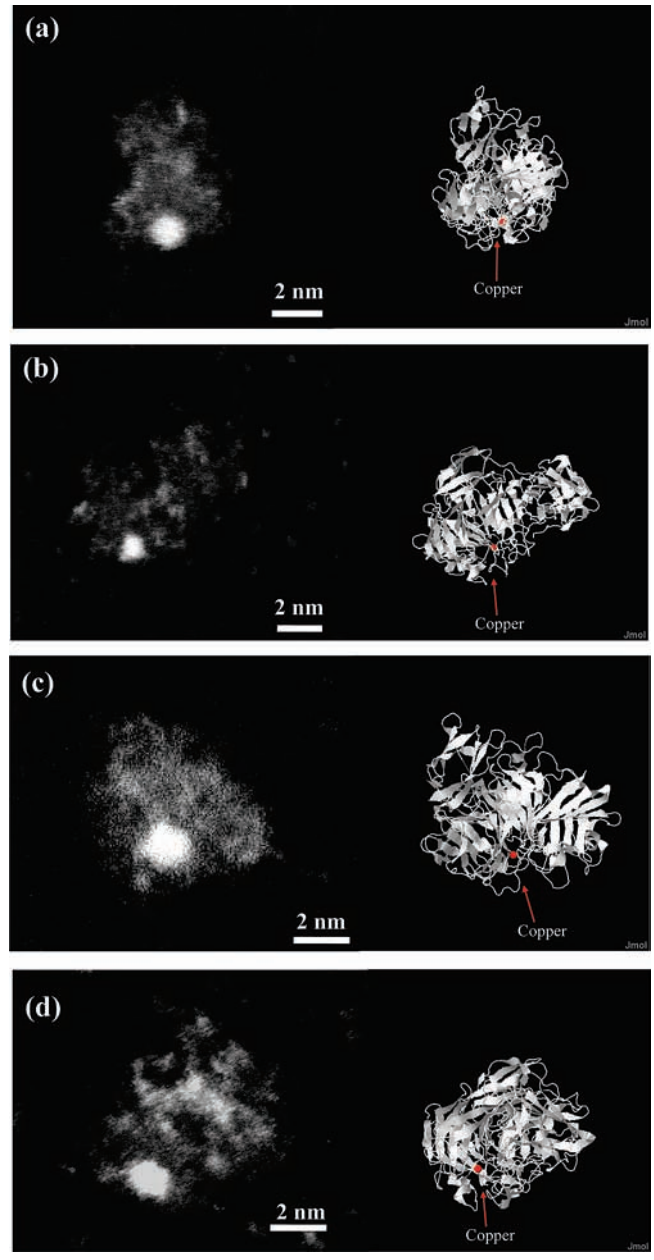

Figure 3. HAADF-STEM images for the coupling of nanoparticles to the protein. (a−d) HAADF-STEM images for TA-AuMPCs−GOase hybrid systems. 3D molecular displays of the protein in different orientations, obtained from Jmol as in Figure 2, are also shown. The cluster is present in the area of the pocket with the copper center, as indicated by the arrows in each image.

To demonstrate the specific binding of the cluster capping ligand to the metal center, TA-AuMPCs were incubated with GOase in solution and further deposited on a TEM grid for analysis. HAADF-STEM images of the material obtained and their comparison with the protein structure from molecular modeling are depicted in Figure 3 for different orientations to highlight the similarities between the images obtained and the molecular model.[12a]

(20) (a) Wang, Y.; Kaifer, A. E. *J. Phys. Chem. B* **1998**, *102*, 9922–9927. (b) Madoz, J.; Kuznetzov, B. A.; Medrano, F. J.; Garcia, J. L.; Fernandez, V. M. *J. Am. Chem. Soc.* **1997**, *119*, 1043–1051.
(21) Hostetler, M. J.; Wingate, J. E.; Zhong, C.-J.; Harris, J. E.; Vachet, R. W.; Clark, M. R.; Londono, J. D.; Green, S. J.; Stokes, J. J.; Wignall, G. D.; Glish, G. L.; Porter, M. D.; Evans, N. D.; Murray, R. W. *J. Am. Chem. Soc.* **1998**, *14*, 17–30.
(22) Daniel, M.-C.; Astruc, D. *Chem. Rev.* **2004**, *104*, 293–346.

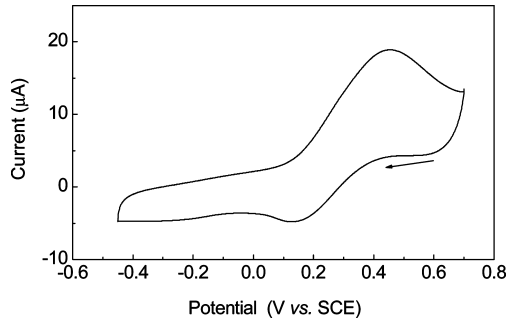

Figure 4. Cyclic voltammogram of a bare gold electrode after incubation for 1 h in a 1 mg/mL GOase protein solution in 20 mM MES buffer, pH 5.1. Measurement was carried out in nitrogen-saturated 20 mM MES buffer pH 7.5 and at a scan rate of 20 mV/s.

These images show that only one cluster is coupled per protein molecule, and by comparison with the molecular modeling structures, it can be concluded that a cluster is attached to the protein at the copper metal site region. It is proposed that this occurs by displacement of the labile H_2O molecule on the Cu^{II} center by the carboxylic groups present on the cluster since X-ray diffraction has confirmed that acetate is able to access the active site and coordinate by displacing H_2O at the substrate binding site.[12a,16] No structural changes of the active site region have been observed when the labile water is replaced by acetate.[12a,c] In addition, the images presented show that no significant unfolding of the protein in the active site region appears to take place. These results demonstrate that it is possible to access the metal center of the metalloenzyme by a coordinative recognition reaction of the $-COO^-$-terminated ligand of the gold clusters. If electrostatic interactions with positively charged amino acids residues along the protein had been involved, clusters attached to different parts of the protein would have been observed.

3.3. Electrochemistry of the AuMPC−GOase Hybrid. Incubation of a bare gold electrode with GOase (Figure 4) resulted in an electrochemically irreversible response as a consequence of an incorrect protein alignment, lack of accessibility of the metal center requiring long rate electron tunneling, or the strong interaction with the gold surface and presumably subsequent protein denaturing. This behavior is in agreement with that previously observed for the reduction of GOase in a capillary gold electrode.[1g]

Following the strategy described in Figure 1b, the protein was immobilized on a gold surface modified with TA-AuMPCs in order to investigate direct ET across the hybrid structure. A gold electrode was first modified with a SAM of biphenyl-4,4′-dithiol to provide a suitable $-SH$ terminus for anchoring the clusters. The presence and integrity of the monolayer after its functionalization were verified by the electrochemical reductive desorption of the attached layer using cyclic voltammetry in basic media.[23]

Figure S3 (Supporting Information) shows the characteristic peak at 1.28 V associated with the reductive desorption of the thiol. A surface thiol coverage of 4.5×10^{14} molecules cm^{-2} ($(7.5 \pm 2) \times 10^{-10}$ mol cm^{-2}) was estimated from the charge under the reductive desorption peak assuming a value of 1 electron per sulfur atom. This value is in agreement with the typical surface density of molecules reported for the maximum thiol coverage on a gold surface.[24]

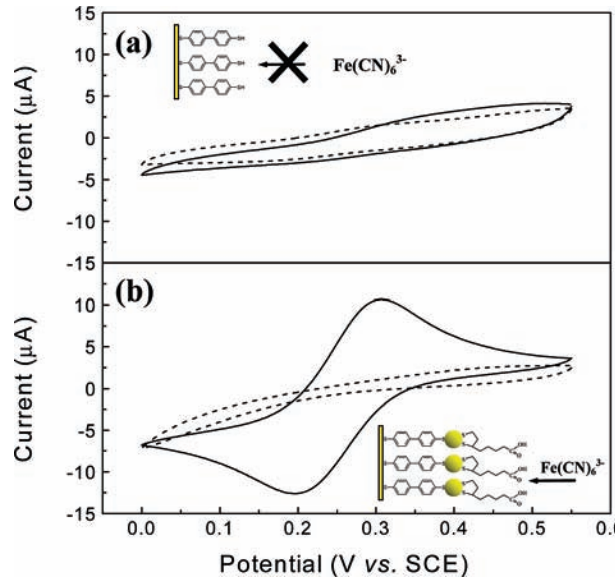

Figure 5. Cyclic voltammograms of a gold electrode modified with SAMs of (a) biphenyl-4,4′-dithiol and (b) biphenyl-4,4′-dithiol-[TA-AuMPCs] (b) and in the presence of 1 mM of ferricyanide in 1 M KCl, pH 3 (solid line) and pH 7.5 (dashed line). Scan rate, 10 mV/s.

The coverage of the electrode by the SAM was also ascertained employing $Fe(CN)_6^{3-}$ as an electrochemical probe, which provides information on the compactness of the monolayer and the presence of functional groups.[20b] No electrochemical response was observed, showing the complete blocking of the surface by the attached SAM (Figure 5a)[25] and demonstrating that this layer is almost defect-free. By contrast, there is evidence of ET after reaction of the dithiol-modified gold electrode with TA-AuMPCs. The cyclic voltammetry of $Fe(CN)_6^{3-}$ depends on the degree of ionization of the carboxylate groups, while at pH 3, where the TA groups are protoned, a reversible faradaic response for the ferricyanide anion is observed. The electrochemical response is completely suppressed at pH 7.5 (Figure 5b). These results are in agreement with a pK_a of 6.5 for TA attached to Au and confirm the attachment of the TA-nanoparticles on the dithiol-gold-modified electrode.[8a,20]

Incubation with GOase of the electrode modified only with the dithiol-SAM did not result in any response different from the background (Figure 6), indicating that the SAM prevents nonspecific protein attachment on the gold surface.

In contrast, incubation of the TA-AuMPCs-modified electrode with GOase solution resulted in the immobilization of the enzyme by coordination with the $-COO^-$-terminated cluster ligands. The reaction was carried out at pH 5.1 to ensure that the Cu^{II} center was coordinated by H_2O instead of OH^- since the pK_a of coordinated H_2O is 5.7.[16] The carboxylate groups of the modified clusters is, therefore, partially protonated at a pH of 5.1, thus avoiding electrostatic repulsion by the attached OH^-.

Figure 7A shows the cyclic voltammograms at 20 mV/s for the modified electrode before (black line) and after incubation

(23) Walczak, M. M.; Popenoe, D. D.; Deinhammer, R. S.; Lamp, B. D.; Chung, C.; Porter, M. C. *Langmuir* **1991**, *7*, 2687–2693.
(24) Love, J. C.; Estroff, L. A.; Kriebel, J. K.; Nuzzo, R. G.; Whitesides, G. M. *Chem. Rev.* **2005**, *105*, 1103–1170.
(25) Saby, C.; Ortiz, B.; Champagne, G. Y.; Bélanger, D. *Langmuir* **1997**, *13*, 6805–6813.

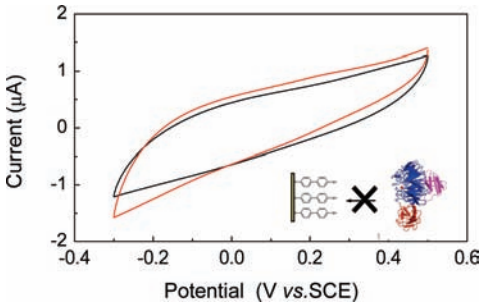

Figure 6. Cyclic voltammogram of a gold electrode modified with a SAM of biphenyl-4,4′-dithiol in a 20 mM nitrogen-saturated MES buffer, pH 7.5, before (black line) and after incubation for 1 h in a 1 mg/mL GOase protein solution (red line) in 20 mM MES buffer at pH 5.1. Scan rate, 20 mV/s.

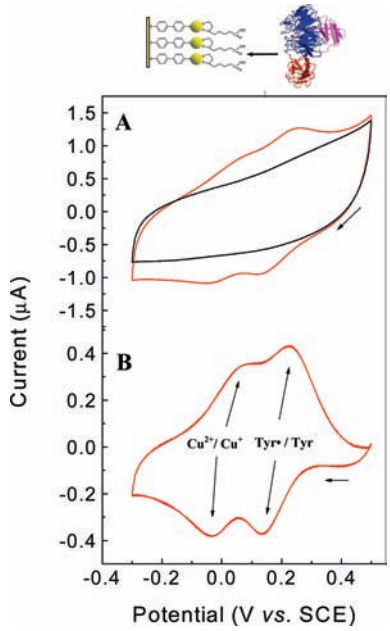

Figure 7. (A) Cyclic voltammograms of a gold electrode modified with a SAM consisting of biphenyl-4,4′-dithiol and carboxylate-gold clusters before (background, black line) and after incubation in GOase protein solution (red line). (B) Cyclic voltammogram after background voltammogram subtraction. Measurements were carried out in nitrogen-saturated 20 mM MES buffer, pH 7.5. Scan rate, 20 mV/s.

(red line). A well-defined direct ET to the enzyme is observed, as shown by the appearance of two voltammetric peaks associated with the two one-electron reactions of GOase (Scheme 1). The redox peaks become clearer after background subtraction (Figure 7B), and these are ascribed to the oxidation/reduction of the tyrosyl radical and to the Cu^{II}/Cu^{I} redox couple, respectively.[13d,14,15a] The hybrid system showed good stability for periods from several hours to a day. These are important results, demonstrating that the protein shows direct ET through the molecular wire consisting of the organic tether−cluster−ligand−protein hybrid system, which facilitates electrical communication and electron relay between the electrode and the metal center. In addition, comparison of Figures 4, 6, and 7 clearly indicates the absence of denaturing.

The surface coverage by the enzyme was estimated from the charge associated with the cyclic voltammetry of the protein film to be 14 ± 0.4 pmol cm^{-2}. These results indicate the presence of a close-packed monolayer of GOase immobilized on a nanostructured surface.

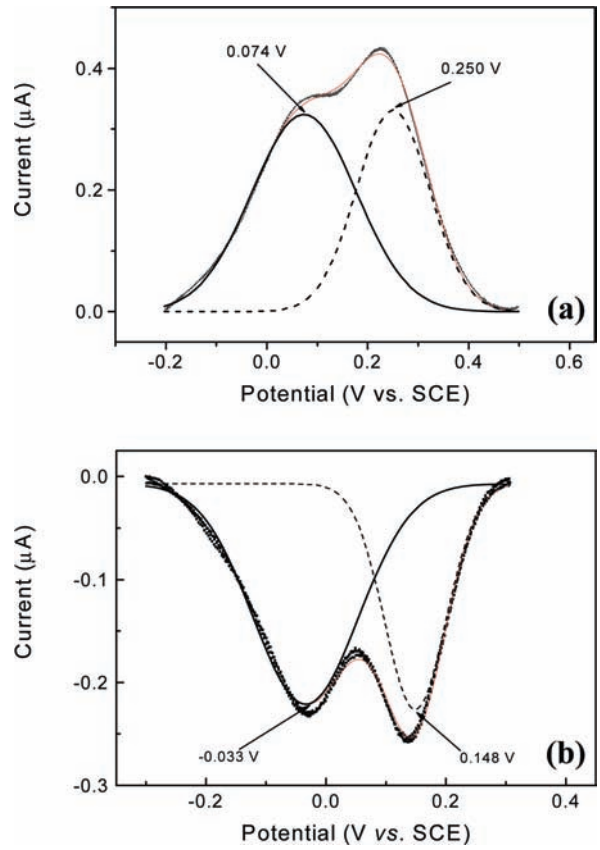

Figure 8. Deconvolution of the voltammetric waves from the electron transfer of galactose oxidase (Figure 7) using Gaussian functions: (a) oxidation wave and (b) reduction wave.

3.4. Formal Potential of the GOase Redox Processes. In order to make a more accurate estimate of the peak potentials of the two processes shown in Figure 7, voltammetric waves were deconvoluted using Gaussian functions, and the results are shown in Figure 8.

From the deconvolution of the voltammograms of five different experiments, the approximate formal potentials $E^{\circ\prime}$ for the two ET processes observed are 196 ± 5 and 21 ± 5 mV. Values previously reported for this protein in solution are 156 and −94 mV vs SCE at pH 7.5,[13d,14,15a] and hence a positive shift in the reduction potential of the tyrosyl radical and the Cu^{II} metal ion is apparent.

Substitution of the exogenous ligand was not expected to have a large effect on the potential of the tyrosyl radical since, for example, its replacement by azide has little effect on the $GOase_{ox}/GOase_{semi}$ potential (149 mV) in solution.[14] Furthermore, changes in the tyrosine redox potential associated with structural modifications of the active site are unlikely, as demonstrated by EXAFS when water remains coordinated to the exogenous site.[26a] However, Rogers et al.[26b] have recently investigated the role of the stacking tryptophan W290, a second-coordination sphere residue, in the stability of the tyroxyl radical. They have pointed out that W290 plays a significant role in

(26) (a) Knowles, P. F.; Brown, R. D.; Koenig, S. H.; Wang, S.; Scott, R. A.; McGuirl, M. A.; Brown, D. E.; Dooley, D. M. *Inorg. Chem.* **1995**, *34*, 3895–3902. (b) Rogers, M. S.; Tyler, E. M.; Akyumani, N.; Kurtis, C. R.; Spooner, R. K.; Deacon, S. E.; Tamber, S.; Firbank, S. J.; Mahmoud, K.; Knowles, P. F.; Phillips, S. E. V.; McPherson, M. J.; Dooley, D. M. *Biochemistry* **2007**, *46*, 4606–4618. (c) Wachter, R. M.; Branchaud, B. P. *J. Am. Chem. Soc.* **1996**, *118*, 2782–2789.

controlling the redox potential of the free radical site. W290 can interact by hydrogen bonding with the acetate copper ligand or with the substrate D-galactose, in agreement with model studies[11b,26c] related to the stability and the formal potential of the radical. The difference of 40 mV observed between the redox potential of the tyrosine radical in solution and immobilized on the surface could be associated with the interaction between the carboxylate groups present at the cluster surface with the W290 or due to confinement effects.[27]

In the case of the Cu^{II}/Cu^{I} couple, a considerable shift of 115 mV in $E^{\circ\prime}$ is observed. This could be associated with differences in the local dielectric permittivity between reaction in solution and at a surface or, most likely, due to local coordination effects caused by the exchange of the ligand on the copper center from water to the carboxylate group, the latter stabilizing the Cu^{I} formed.

It is known that the redox potential of metalloenzymes can be modified over a broad range of values by distortion of the coordination geometry,[13c,28] which can occur when the metal center is forced into an unusual geometry constrained by the protein-stable entatic state.[29] The rigidity of the redox site, caused by the GOase protein fold, favors the distorted square-pyramidal geometry of the Cu^{II} over the tetrahedral or square-planar geometry of the Cu^{II}.[13c,30] It has been proposed that, on reduction, the Cu^{I} species becomes three-coordinate, with a planar geometry, due to the displacement of the tyrosine Tyr495 group and of the water molecule. The coordination environment then consists of two histidine imidazole groups and the modified tyrosine residue (His496, His581, and Tyr272, Figure 1).[26a,10b,11b,13c] In the present system, however, the coordinated carboxylate ligand could remain coordinated to Cu^{I}, with only the tyrosine Tyr495 group being displaced. This would lead to a stable four-coordinate geometry with Cu^{I}, thus making the reduction of Cu^{II} more favorable and, hence, shifting the reduction potential to more positive values, as observed.

The dependence on pH of $E^{\circ\prime}$ for the radical was measured, and a linear relationship with a slope close to -60 mV/pH was obtained for the Cu^{II}-$Tyr^{\bullet}$ ($GOase_{ox}$)/Cu^{II}-Tyr^{-} ($GOase_{semi}$) redox couple (Figure S4, Supporting Information). This corresponds to a reversible one-electron, one-proton reaction, in agreement with previous observations.[13d,14,15] This pH dependence has been associated with the protonation of the axial Tyr495 group, with a pK_a of 6.7.[16,31] Similar to previous reports,[13d,14,15] the redox potential values for the tyrosyl radical are more negative than those observed for other tyrosyl radical systems in a non-protein matrix, for which the TyrO$^{\bullet}$/TyrOH couple ranges from 0.54 to 0.76 V vs SCE.[32] These results highlight the known importance of the protein environment in tuning redox potentials. It is proposed that the decrease in potential is a consequence of the coordination of the phenolate anion of Tyr272 to the Cu^{II} center. Additional stabilization results from the thioether bond between tyrosine and a cysteine residue (Cys228) cross-linked at the ortho position of the phenolate anion and from the protection of this bond by the indole ring of the tryptophan residue Trp290.[12a,13e]

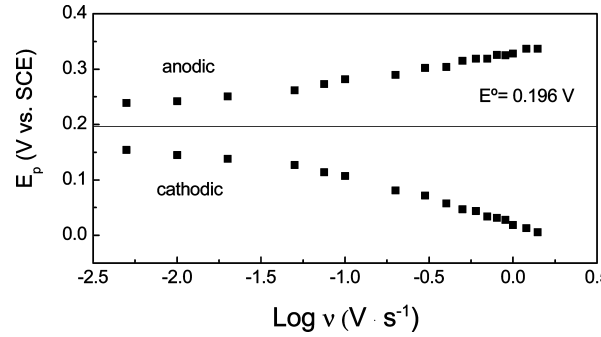

Figure 9. Plot of anodic and cathodic peak potential against the logarithm of the scan rate.

3.5. Rate Constants for Electron Transfer to the GOase Enzyme. The dependence of the cyclic voltammetry on scan rate is shown in Figure S5 (Supporting Information). At low scan rates, the ratio of peak current to scan rate is approximately constant for the tyrosyl radical peak, and those for the Cu^{II}/Cu^{I} redox couple are well-developed.

The tyroxyl radical is very stable, with a half-life of nearly 1 week in the absence of reductants.[11a] This stability arises from delocalization of the unpaired electron of the Tyr-Cys group over Tyr495 and the shielding of the radical complex from the solvent by the tryptophan residue (W290).[12a,13e,31]

The redox properties of this unusually stable tyrosyl radical were further investigated. At higher scan rates, a deviation from linearity of the peak current I_p with respect to the sweep rate (v) is observed for $v > 100$ mV/s (Figure S6, Supporting Information).

The heterogeneous ET rate constant (k_{sh}) for the tyrosyl radical reaction was calculated using Laviron's method,[33] from the sweep rate dependence of the peak-to-peak separation between the reduction and oxidation waves of the tyrosyl radical (Figures 9 and S7, Supporting Information); $\alpha = 0.37 \pm 0.03$ and $k_{sh} = 0.9 \pm 0.2$ s^{-1} were found for $\Delta E_p > 200/n$ mV. Also, k_{sh} was calculated for $\Delta E_p < 200/n$ mV,[33] and an approximate value of $k_{sh} = 0.6$ s^{-1} (Figure S8, Supporting Information) was obtained.

These results show a high ET rate of the hybrid system for the reduction of the tyrosyl radical through the cluster to the electrode and that this rate is not determined by the properties of the hybrid junction. Thus, excellent electrical communication between the redox center and the electrode is achieved using the approach described in the present work.

The Cu^{II}/Cu^{I} redox process shows a very different behavior, with a very rapid decrease of the peak current with sweep rate. This behavior corresponds to a chemical−electrochemical process, and this could be ascribed to the significant changes in the active-site structure discussed above, leading to a change in the copper ion coordination number on reduction. From the above, the rate constants for the two redox couples in GOase are very different. The radical reaction is very fast, whereas the reduction of the metal center is slow, and a value for the rate constant could not be estimated from the present results. The difference between these two processes lies in their reorganization energies. The ET to the radical corresponds to a

(27) Behera, S.; Raj, C. R. *J. Electroanal. Chem.* **2008**, *619−620*, 159–163.
(28) (a) Vallee, B. L.; Williams, R. J. P. *Proc. Natl. Acad. Sci. U.S.A.* **1968**, *59*, 498–505. (b) Ryde, U.; Pierloot, O. K.; Roos, B. O. *J. Mol. Biol.* **1996**, *261*, 586–596. (c) Ghosth, P.; Shabat, D.; Kumar, S.; Sinha, S. C.; Grynszpan, F.; Li, J.; Noodleman, L.; Keinan, E. *Nature* **1996**, *382*, 339–341.
(29) Williams, R. J. P. *Eur. J. Biochem.* **1995**, *234*, 363–381.
(30) Jazdzewski, B. A.; Tolman, W. B. *Coord. Chem. Rev.* **2000**, *200−202*, 633–685.
(31) Wright, C.; Sykes, A. G. *Inorg. Chem.* **2001**, *40*, 2528–2533.
(32) (a) DeFelippis, M. R.; Murthy, C. P.; Broitman, F.; Weinraub, D.; Faraggi, M.; Klapper, M. H. *J. Phys. Chem.* **1991**, *95*, 3416–3419. (b) DeFelippis, M. R.; Murthy, C. P.; Faraggi, M.; Klapper, M. H. *Biochemistry* **1989**, *28*, 4847–4853.
(33) Laviron, E. *J. Electroanal. Chem.* **1979**, *101*, 19–28.

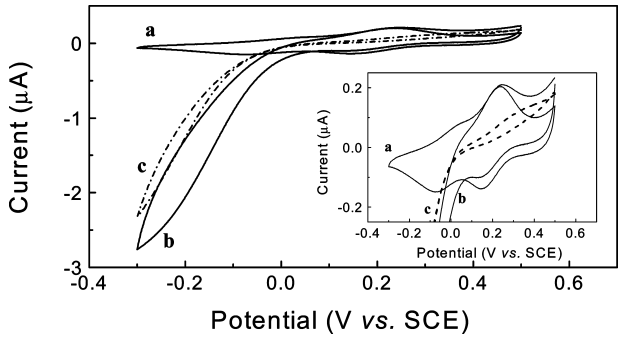

Figure 10. Cyclic voltammograms of a gold electrode modified with a SAM consisting of biphenyl-4,4′-dithiol-[TA-AuMPCs] after incubation with a solution of GOase (a) in the absence of oxygen, where the redox states for the protein are observed (inset), and (b) in the presence of oxygen. (c) Control experiment for the same modified gold electrode in the absence of the protein and in the presence of oxygen. Measurements were carried out in 20 mM MES buffer, pH 7.5. Scan rate, 20 mV/s.

charge-delocalized system, whereas that to the Cu^{II} species involves a large structural reorganization of the ligand environment and site geometry. This enzyme has an unusual combination of two different ET sites, one localized and one delocalized, and the present results clearly demonstrate this dual characteristic of GOase.

3.6. Oxygen Reduction Catalyzed by the AuMPC−GOase Hybrid. The electrocatalytic reduction of oxygen as an electron acceptor for the GOase/TA-MPCs/Au-electrode system was also studied. This reaction has been reported to be very fast, with a rate constant of 1.01×10^7 M^{-1} s^{-1}.[11e] Its mechanism is not well understood.[10a−c,11b,e] Reoxidation of the enzyme occurs by electron and proton transfers to oxygen, and it has been proposed that a Cu^{I} species acts as the coordination center, leading to formation of hydrogen peroxide.[11b,e]

Figure 10 shows the cyclic voltammograms of the hybrid system in the absence (curve a) and presence (curve b) of oxygen. In the absence of oxygen, the reversible redox reactions of the protein can be clearly observed. By contrast, oxygen reacts with the Cu^{I} species, giving rise to a large electrocatalytic reduction current at potentials close to the reduction potential of the Cu^{II}/Cu^{I} couple, with the simultaneous disappearance of the oxidation peak as would be expected for an EC mechanism. It is interesting to notice that no electrocatalytic response is observed for the tyrosyl radical reduction process, in agreement with the lack of reactivity reported for oxygen reduction by the semireduced form ($GOase_{semi}$, Cu^{II}-Tyr) obtained by reduction of the tyroxyl radical.[10a] If spin is delocalized and there is no coordination center for the O_2 molecule, as appears to be the case with the tyrosyl moiety of GOase, the reactivity is low. For this reason, the reduction of oxygen is observed only when a coordination center is created by reduction of Cu(II) to Cu(I). An example of this, although in a different context, has been recently published employing quantum chemical calculations to describe the reactivity of oxygen with semiquinone radicals.[34]

For comparison, a control experiment for the TA-MPCs/Au-electrode system in the presence of oxygen is included in Figure 10(curve c). Although the gold clusters can also show catalytic activity for oxygen reduction,[22] in the presence of protein the onset potential shifts ~80 mV to more positive values, corresponding to the potential of the Cu^{II}/Cu^{I} couple. These results indicate that the immobilized GOase retains its catalytic activity for oxygen reduction.

Catalytic oxidation of the natural substrate D-galactose is not observed in the absence of oxygen (data not shown). The experiment was carried out by conducting an anodic scan to obtain Cu^{II}-$Tyr^{\bullet}$ ($GOase_{ox}$) species to react with galactose present at a concentration of 175 mM (the value of the Michaelis−Menten constant, K_M, of galactose[11a,35] at which half-maximal rate is observed) at pH 7.5. This result is to be expected since the substrate binding site of the metal center should be blocked by the attachment of the cluster through its carboxylate termination, thus hindering the binding of galactose.

It has been demonstrated that galactose binds at the exogenous position, but the coordination position for oxygen remains unclear.[10a−c,11] The absence of catalytic response for galactose but not for oxygen reduction suggests that the latter binds to copper in a different position from that of galactose.[31] Although the oxidation of galactose is inhibited by the attachment of the molecular wire described in this work, the reduction of oxygen is not affected, indicating that the oxygen molecule does not compete for the exogenous position in the active site. The coordinative binding strategy presented in this work can be employed for other metalloenzymes for which the coordinative position replaced is not involved in the binding substrate site.

Conclusions

The binding of Au clusters to the metal center of the metalloenzyme galactose oxidase has been demonstrated, and it has been shown that this establishes electrical contact between an electrode and the enzyme. This results in fast direct electron transfer, facilitated by the coordination of its metal center site to the ligands in the gold cluster. The hybrid system showed also an effective electrocatytic response for oxygen reduction. This methodology could be extended to other metalloenzymes, preserving their natural enzymatic activities and enhancing ET rates. Furthermore, gold clusters can be functionalized with other specific coordinative ligands to promote DET and to modify the formal potential and the catalytic properties of the protein. Future applications could include the development of third-generation (mediatorless) biosensors, bioelectronic applications as devices at the nanoscale, and applications in biofuel cells. Finally, the HAADF-STEM technique has been shown to be a powerful tool for protein imaging.

Acknowledgment. The financial support from the EU under the DYNAMO project is gratefully acknowledged. We are grateful to Dr. Simon Romani for STEM measurements, Prof. Simon Phillips for help with the protein models, and Mr. Stephen Apter for help with the elemental analyses.

Supporting Information Available: HAADF-STEM images and UV−visible spectrum of TA-capped gold clusters (Figures S1, S2); reductive desorption cyclic voltammogram of a gold electrode modified with a SAM of biphenyl-4,4′-dithiol (Figure S3); linear relationship of standard potential on solution pH (Figure S4); cyclic voltammograms at different scan rates (Figure S5); plot of cathodic peak current versus scan rate and Laviron's plot for Cu^{II}-$Tyr^{\bullet}$/Cu^{II}-Tyr^{-} system (Figures S6, S7, S8). This material is available free of charge via the Internet at http://pubs.acs.org.

JA9026693

(34) Wass, J. R. T. J.; Ahlberg, E.; Panas, I.; Schiffrin, D. J. *Phys. Chem. Chem. Phys.* **2006**, *8*, 4189–4199.

(35) Kwiatkowski, L. D.; Adelman, M.; Pennely, R.; Kosman, D. J. *J. Biol. Inorg. Chem.* **1997**, *2*, 209–222.